Numerical Computations of Resistance for Japan Bulk Carrier in Calm Water

Tao Sun (Shanghai Jiao Tong University, State Key Laboratory of Ocean Engineering, Collaborative Innovation Center for Advanced Ship and Deep-Sea Exploration, China)
Chonghong Yin (Shanghai Jiao Tong University, State Key Laboratory of Ocean Engineering, Collaborative Innovation Center for Advanced Ship and Deep-Sea Exploration, China)
Jianwei Wu(Shanghai Jiao Tong University, State Key Laboratory of Ocean Engineering, Collaborative Innovation Center for Advanced Ship and Deep-Sea Exploration, China)
Decheng Wan*(Shanghai Jiao Tong University, State Key Laboratory of Ocean Engineering, Collaborative Innovation Center for Advanced Ship and Deep-Sea Exploration, China)
***Corresponding author: dcwan@sjtu.edu.cn**

1. SUMMARY

Resistance prediction for a ship is one of the vital tasks at the design stage. In this paper, the in-house multifunction solver naoe-FOAM-SJTU based and developed on the open source code OpenFOAM is applied to study the resistance, sinkage & trim characteristics and the local flow around the stern of Japan Bulk Carrier (JBC) with and without an energy saving device named wake equalizing duct (WZD) sailing in calm water. A V&V method is used to determine the errors and uncertainties. The numerical results of the presented paper agree very well with the measurement data of model test.

2. INTRODUCTION

Resistance predictions for a ship is one of the most important tasks at the design stage in order to ensure that ship can sail at a desired speed with the installed engine capacity and fulfill the mandatory regulations imposed by IMO such as Energy Effiency Design Index(EEDI). Since new concerns on environment and efficiency have risen in recent decades, predictions are getting more important and as a result the interests on Energy Saving Device (ESD) increased significantly. Wake equalizing duct (WED), studied in this paper, is one of the most commonly used energy saving devices for improving the propulsion performance of a ship and reducing the propeller-excited vibrations and viscous resistance forces, especially suitable for vessels with fat stern such as bulk carrier and oil tanker. Wake equalizing duct is fitted in stern before propeller, the general function of it is set to improve uniformity of propeller's inflow field, thus homogenizing the wake and improving hull efficiency. Also, the wake equalizing duct can accelerate the flow by means of the lift created by the aerofoil shape of the duct cross-section.

There are three different ways to predict resistance. Empirical methods are the simplest and fatsest among them. Another tool for predictions is model testing which is the most reliable and accurate method. Alternative to model tests and the last method of prediction is numerical simulation. Among them, CFD method shows a huge advantage and has gained popularity in the past decades due to a more physics-based modeling, capability of handling non-linear free-surface, especially for detail presentation of flow fields, which is important to study the effect of energy saving devices.

In this paper, the in-house multifunction solver naoe-FOAM-SJTU was applied to simulate the viscous flow field and compute the resistances of Japan Bulk Carrier with and without an energy saving device. In addition, a formal Verification and Validation (V&V) method is applied to control and understand the modelling and numerical errors in the computations. Based on OpenFOAM, the in-house solver naoe-FOAM-SJTU is appropriate for various kinds of complex hydrodynamic issues of naval architecture and ocean engineering. Previous works have made many progresses in developing and validating this solver applied in this paper. In 2011, Cha and Wan firstly accomplished the numerical wave generation and absorption. Shen and Wan simulated the viscous flow acting on KVLCC2, KCS, and DTMB5415 and compared with the measurement results by naoe-FOAM-SJTU. Ye and Wan (2012) computed the added resistance in regular head waves with ship trim and sinkage, and validated the ability of naoe-FOAM-SJTU to solve the strongly nonlinear problems. Cao and Wan (2012) studied the extreme wave effects on cylindrical offshore structures by naoe-FOAM-SJTU. Liu and Wan used naoe-FOAM-SJTU to simulate motion responses of an offshore observation platform in regular waves.

However, there is no guarantee that computed results will match with the.] physical reality. Therefore a systematic approach should be used in order to determine the quality of merhod. V&V method is applied in this paper to determine the errors and uncertainties.

The paper is organized as follows. The description of computational methods is presented first, and is followed by the geometry and overset mesh. The results are then presented and discussed. Finally, a summary and conclusions are provided.

3. COMPUTATIONAL METHODS

In the simulation of unsteady incompressible viscous two-phase flow field, the Reynolds-Averaged Navier-Stokes (RANS) equations are applied in this paper as governing equations. The equations of continuity and momentum equation can be written as

$$\nabla \cdot \boldsymbol{U} = 0 \tag{1}$$

$$\frac{\partial \rho \boldsymbol{U}}{\partial t} + \nabla \cdot (\rho(\boldsymbol{U} - \boldsymbol{U}_g)\boldsymbol{U}) = -\nabla p_d - \boldsymbol{g} \cdot x \nabla \rho + \nabla \cdot (\mu_{\mathbf{eff}} \nabla \boldsymbol{U}) + (\nabla \boldsymbol{U}) \cdot \nabla \mu_{\mathbf{eff}} + f_\sigma + f_s \tag{2}$$

in which, $\boldsymbol{U}$ stands for the velocity field while $\boldsymbol{U}_g$ means velocity of mesh points; p_d is dynamic pressure, whose value is equal to total pressure subtracting hydrostatic component; ρ is mixed density of the two phases; $\boldsymbol{g}$ is the gravitational acceleration; μ_{eff} is the effective dynamic viscosity computed by (ν+ν_t), where ν is kinematic viscosity coefficient and ν_t is eddy viscosity; f_σ is a surface tension term, which impacts the free surface. To protect the flow field from the interface of echo waves, the source term f_s is added to generate a sponge layer to absorb the generated wave.

The SST *k-w* model is applied as the turbulence model in this paper. This turbulence model synthesizes the advantages of standard *k-w* model and *k-epsilon* model. The former one is appropriate to simulate the turbulent flow far away the wall plane, while the latter is good at handling the boundary flow near the wall under different pressure gradients. The accuracy of numerical computation is satisfactory by using the SST *k-w* turbulence model.

The volume of fluid (VOF) method with artificial compression technique is applied for locating and tracking the free surface (Hirt and Nichols,1981). In the VOF method, each of the two-phase is considered to have a separately defined volume fraction (α), where 0 and 1 represent that the cell is filled with air and water respectively and $0 < \alpha < 1$ stands for the interface between two-phase fluid. The density and dynamic viscosity for the mixed fluid can be presented as:

$$\begin{aligned} \rho &= \alpha \rho_1 + (1-\alpha)\rho_2 \\ \mu &= \alpha \mu_1 + (1-\alpha)\mu_2 \end{aligned} \tag{3}$$

The volume fraction function can be determined by solving an advection equation:

$$\frac{\partial \alpha}{\partial t} + \nabla \cdot \left[\left(\boldsymbol{U} - \boldsymbol{U}_g \right) \alpha \right] + \nabla \cdot \left[\boldsymbol{U}_r (1-\alpha) \alpha \right] = 0 \tag{4}$$

where the last term on the left-hand side is an artificial compression term to limit the smearing of the interface and $\boldsymbol{U}_r$ is a relative velocity used to compress the interface.

The Finite Volume Method (FVM) is used to discretize both the RANS equations and VOF transport equation in naoe-FOAM-SJTU. According to FVM, the computational domain is partitioned into grid cells and each grid node is surrounded by a control volume. Field information is stored at the center of cells. Then cell center values are interpolated into face values, which are summed to compute the volume integration. Different interpolation schemes are applied. In detail, a second-order TVD limited linear scheme is used to discretize the convection terms in Eq.(2); the diffusion terms are discretized by a second-order central difference scheme; the van Leer scheme is applied for VOF equation discretization; a second-order backward method is applied for temporal discretization.

For the discretized RANS equations, the PISO (pressure-implicit-split-operator) algorithm is adopted to solve the coupled equation of velocity and pressure. Each PISO loop contains three steps, namely prediction, correction and second correction. The second correction can make velocity and pressure correspond with the momentum equation and continuity equation more effectively so that the convergence of each loop is accelerated.

4. GEOMETRY AND MESH

4.1 JBC model

JAPAN Bulk Carrier (JBC) is a Capesize bulk carrier designed by National Maritime Research Institute (NMRI), Yokohoma University, Ship Building Research Centre of Japan (SRC) and with the support of ClassNK. Ship is equipped with a wake equalizing duct as an energy saving device. The wake equalizing duct consists of duct and duct strut.

In this paper, wake equalizing duct equipped in a low-speed full form ship in model scale is studied, and results of computations and investigations will be presented for resistance. The wake equalizing duct model is shown in Fig. 2, which is an effective energy saving device that have been devised especially for the ships with large block coefficients and fat stern like JBC to improve the propeller performance. The general function of the wake equalizing duct is set to

work against the asymmetry of wake and reduce the flow separation to recover hull surface pressure at stern.

Main dimensions and particulars of JBC are listed in Table 1, including both the full scale and the model scale. The 3D models of hulls with and without wake equalizing duct are shown in Fig. 3, including the stern and overall hull. In order to obtain a mesh with good quality, the sides of hull deck is rounded off.

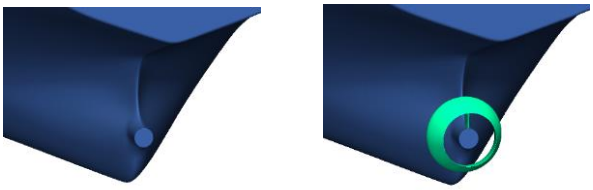

(a) Bare JBC hull (b) hull with ESD

Fig.2 Computational models of JBC for resistance (a, b)

Table 1 Principle Dimensions of JBC

Main particulars	Full scale	Model scale
L_{PP} (m)	280	7
L_{WL} (m)	285	7.125
B_{WL} (m)	45	1.125
D (m)	25	0.625
T (m)	16.5	0.4125
∇ (m^3)	178369.9	2.7870
$S_{0_w/oESD}$ (m^2)	19556.1	12.2226
S_{0_wESD} (m^2)	19633.9	12.2706
C_B	0.858	0.858
C_M	0.9981	0.9981
LCB	2.5475	2.5475
x/L_{PP}	0.985714	0.985714
$-z/L_{PP}$	-0.0404214	-0.0404214

4.2 Case conditions

JBC models were performed at Re=7.46×10^6 and Fr=0.142, corresponding to a velocity of 1.179 m/s (14.5kn for full scale). To compare the numerical simulation with model test, the case conditions are set identically to the model test. The water density is 998.2 kg/m^3 and the kinematic viscosity is 1.107×10^{-6} m^2/s. The value of gravitational acceleration is 9.80 m/s^2.

4.3 Mesh and domain

For numerical computations in this paper, a same computing domain is used. The space coordinate range is determined as $-1.0L_{pp} < x < 4.0L_{pp}$, $-1.5L_{pp} < y < 1.5L_{pp}$, $-1.0L_{pp} < z < 1.0L_{pp}$. The mesh is generated by *SnappyHexMesh*, an automatic mesh generation tool provided by OpenFOAM. This tool generates mesh based on Cartesian grids by splitting hexahedral cells, resulting in unstructured octree-hexahedral grids.

The overall domain mesh and the details near the bow and stern are displayed in Fig.2. The grids of important regions are refined to capture precisely the free surface and the wake flow field, and accurately compute the variables near wall region of the hull. The refinement domains consist of the boundary layer around the hull, the interface region, the area near bulbous bow and the rear of stern. Near 1.0 million cells for a case are generated.

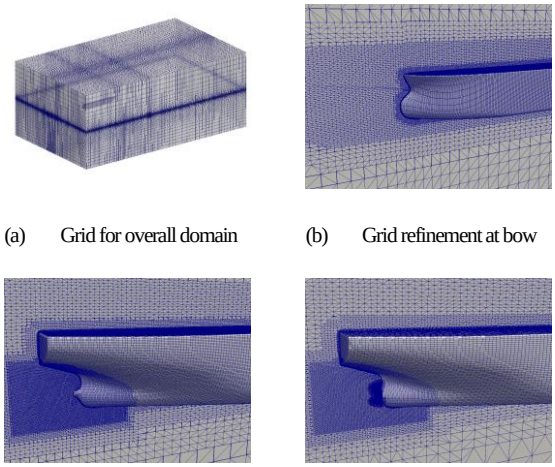

(a) Grid for overall domain (b) Grid refinement at bow

(c) Grid refinement at stern without ESD (d) Grid refinement at stern with ESD

Fig.3 Grid for Japan Bulk Carrier

5. ANALYSIS OF RESULTS

5.1 Verification and Validation

Currently, verification and validation tend to be useful for quantifying numerical and modeling errors in CFD computations, as well as for establishing the credibility of the CFD method and its solution. In practical applications, solution verification estimates the numerical error and uncertainty, in which the most important issue is determining the iterative and discretization error and uncertainty. Although several techniques are available, a so-called grid convergence study is normally used.

Proceded by verification, validation is a process that controlling the numerical solution against the approriate experimental data, in order to reveal the error and uncertainty from both numerical and modellling deficiencies.

This paper is concentrated on bare hull without ESD and hull with ESD, which are Case 1.1a(NMRI) and Case 1.2a(NMRI)

Because the grids of bare hull or hull with ESD don't have much in difference, A grid dependence study is carried out only for hull without ESD with three systematically refined grids. Table 2 shows the grid properties for Case 1.1a(NMRI). A uniform refinement ratio $r=h_{i+1}/h_i=\sqrt{2}$ is applied for all grids in three directions. Grid Properties for Case 1.1a(NMRI) is displayed in Table 2. Grid convergence tendencies of C_T, C_F and C_P and the comparision of resistance coefficients and experimental data are shown in Table 3.

Table 2 Grid properties for Case 1.1a(NMRI)

NO	Grid Cells	h_i/h_1
Coarse Grid	784165	1.414
Medium Grid	1973426	1.414
Fine Grid	4615651	1.414

Table 3 Grid convergence study for Case 1.1a(NMRI)

Parameters		EFD	V&V study			r_G	$\varepsilon_{12}\%S_1$	U_I/ε_{12}	$p_G/p_{G,th}$	$U_G\%S_1$
			Coarse	Medium	Fine					
$C_T\times10^3$	Value	4.29	4.78	4.18	4.27	1.4	2.068	0.073	2.785	7.122
	E%D	/	-11.54	2.63	0.57	/	/	/	/	/
$C_F\times10^3$	Value	/	2.95	2.74	2.82	1.4	2.926	0.079	1.343	3.709
$C_P\times10^3$	Value	/	1.84	1.44	1.45	1.4	0.392	0.003	6.147	13.869
sinkage[%Lpp] upwardpositive	Value	-0.09	-0.08	-0.08	-0.08	1.4	1.446	0.008	1.416	-1.928
	E%D	/	5.81	2.09	3.49	/	/	/	/	/
trim[%Lpp] bow up positive	Value	-0.18	-0.17	-0.17	-0.17	1.4	1.098	0.034	0.610	-0.838
	E%D	/	3.33	4.94	3.89	/	/	/	/	/

a. r_G is grid refinement ratio
b. U_I is the iterative uncertainty
c. U_G is the grid uncertainty
d. $E\%D=(D-S)/D\times100$
e. $\varepsilon_{12}\%S_1=|S_1-S_2)/S_1\times100$

The grid convergence study for C_T, C_F, C_P, sinkage and trim shows that these parameters are of oscillatory iterative convergence. For oscillatory iterative convergence, the deviation of the variable from its mean value provides estimates of the iterative uncertainty based on the range of the maximum S_U and minimum S_L values

$$U_I=\left|\frac{1}{2}(S_U-S_L)\right| \tag{3}$$

The medium grid is applied to the numerical computation for JBC with and without ESD. The total resistance coefficients from CFD computation have error about 2.6% compared with the experimental data. For low-speed JBC without ESD, the friction resistance dominates.

Table 4 Computation validation for Case 1.2a(NMRI)

Parameters		EFD	Medium Grid
$C_T\times10^3$	Value	4.263	4.156
	E%D	/	2.516
$C_F\times10^3$	Value	/	2.734
$C_P\times10^3$	Value	/	1.421
sinkage[%Lpp] upwardpositive	Value	-0.085	-0.084
	E%D	/	0.927
trim[%Lpp] bow up positive	Value	-0.182	-0.174
	E%D	/	4.439

As is shown in Table 4, the total resistance coefficients from CFD computation have error about 2.5% compared with the experimental data. For low-speed JBC with ESD, the friction resisitance dominates. Cp for Case 1.2(NMRI) is smaller than Cp for Case 1.1(NMRI).

5.2 Free surface

The wave pattern generated by the hull system in calm water is a significant factor to affect the ship resistance, especially for the wave making resistance. Because the JBC sails in low speed, so the wave making resistence matters a little in this paper. But the shape of wave form can be an indicator to check whether the computation is

correct or not. As a result, the simulation of free surface is an important aspect to study the resistance performance of JBC. After the steady flow field has been fully formed, the free surfaces of the JBC without and with ESD are captured, as shown in Fig. 4.

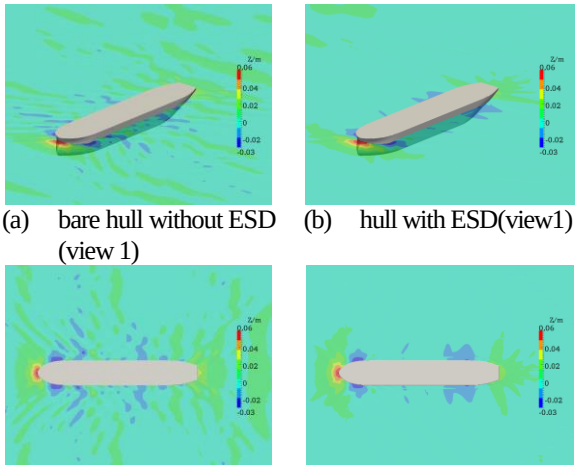

(a) bare hull without ESD (view 1) (b) hull with ESD(view1)

(c) bare hull without ESD(view2) (d) hull with ESD(view2)

Fig.4 Free surface for Japan Bulk Carrier

As is shown in Fig 4, there is a wave crest near the bow and a wave trough near the stern.

5.3 Streamlines near the hull

The information of the interior velocity field is used to draw the streamlines around the hull. By studying the direction and pattern of streamlines, the motion of fluid particles can be investigated and the influence of the flow field on hull can be inferred. The turbulent flow is another important factor for the increase of ship resistance. The streamlines near bow and stern of one hull under different velocity conditions are shown in Fig.5. The contour represents the magnitude of flow velocity

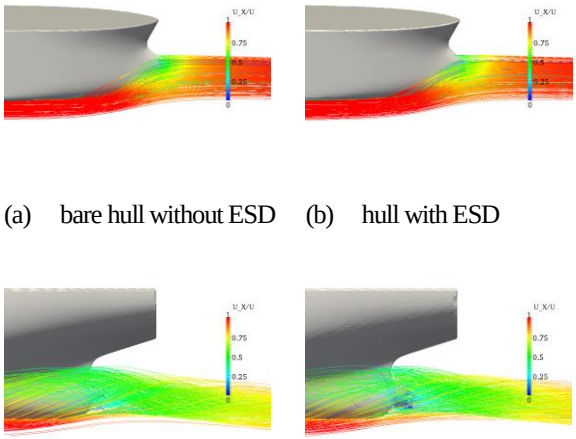

(a) bare hull without ESD (b) hull with ESD

(c) bare hull without ESD (d) hull with ESD

Fig.5 Streamlines near Japan Bulk Carrier

5.4 Wake flow field near the hull

Contours of mean axial velocity at x/L_{pp}= 0.9746 and x/L_{pp}= 0.9843 are shown in Fig. 6. The former cross section is situated before the ESD and the later one is situated at the gap between the propeller and the ESD.

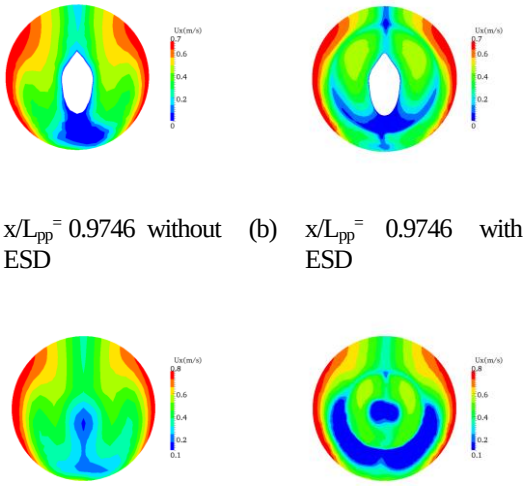

(a) x/L_{pp}= 0.9746 without ESD (b) x/L_{pp}= 0.9746 with ESD

(c) x/L_{pp}= 0.9843 without ESD (d) x/L_{pp}= 0.9843 with ESD

Fig.6 Wake flow field near Japan Bulk Carrier

5.5 Pressure distribution around the hull

The pressure difference between bow and stern leads to viscous pressure resistance. The kinetic energy of water particle is dissipated by viscous effects. The pressure contour on the surface of hull affects the resistance performance as well. The pressure distributions under the water plane around JBC without and with ESD are shown in Fig.6.

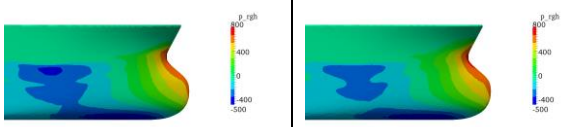	
(a) bare hull without ESD at bow	(b) hull with ESD at bow

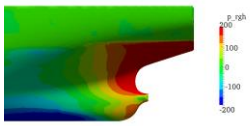	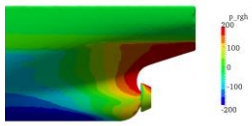
(c) bare hull without ESD at stern	(d) hull with ESD at stern

Fig.7 Pressure distribution

Fig. 7 presents the bow and stern pressure distribution of JBC with and without ESD. It shows that there is a similar pressure distribution at bow between the two ships, but due to the influence of the wake equalizing duct, stern pressure distributions show a great difference between JBC ships with and without ESD. There is an obvious decrease of the low pressure area at the ship stern after installing energy-saving device, which can be beneficial to reduce the pressure resistance. In addition, the low pressure area created in front of the duct can also have positive effects in terms of reattaching separated flow to the hull in the vicinity of the duct. The difference of pressure distribution leads to the difference of viscous pressure resistance between JBC with and without ESD.

6. CONCLUSION

In this paper, numerical simulations focusing on Japan Bulk Carrier (JBC) without and with WSD sailing in calm water at low speed have been performed. A series of factors which affects the sailing performance have been considered. The study contains the calculation of resistance components, comparisons with the test data, free surface, analyses of pressure distribution and streamlines around the hull. Some meaningful conclusions can be summarized.

The RANS solver naoe-FOAM-SJTU is proved to be reliable to handle general fluid hydrodynamic issues with a good efficiency, which is the main purpose of the study in this paper. It has a good extendibility with high efficiency which will be able to solve more complex nonlinear problems in the future.

REFERENCES

KB. KORKMAZ., (2015), CFD Predictions of Resistance and Propulsion for the JAPAN Bulk Carrier (JBC) with and without an Energy Saving Device[M]. Chalmers University of Technology, Gothenburg, Sweden.

Zou, L., & Larsson, L. (2014). CFD Verification and Validation in Practice - AStudy Based on Resistance Submission to the Gothenburg 2010 Workshop on Numerical Ship Hydrodynamics. In 30*th Symposium on Naval Hydrodynamics*. Hobart, Tasmania, Australia.

ZHA Ruosi, YE Haixuan and SHEN Zhirong et al, (2014). Numerical study of viscous wave-making resistance of ship navigation in still water[J]. Journal of Marine Science and Application, 13(2): 158-166.

SHEN Zhirong, YE Haixuan, and WAN Decheng (2012). Motion response and added resistance of ship in head waves based on RANS simulations[J]. Chinese Journal of Hydrodynamics, 27(6): 621-633.

LIU Yuanchuan, WAN Decheng (2013). Numerical simulation of motion response of an offshore observation platform in waves[J]. Journal of Marine Science and Application, 1(12): 89-97.

SHEN Zhirong, WAN Decheng (2013). RANS computations of added resistance and motions of a ship in head waves[J]. International Journal of Offshore and Polar Engineering, 23(4): 263-271.

DHAKAL T., WALTERS D (2009). Curvature and rotation sensitive variants of the K-Omega SST turbulence model[C]. ASME 2009 Fluids Engineering Division Summer Meeting. American Society of Mechanical Engineers.